Proceedings of the ASME 2010 3rd Joint US-European Fluids Engineering Summer Meeting and 8th International Conference on Nanochannels, Microchannels, and Minichannels
FEDSM-ICNMM2010
August 1-5, 2010, Montreal, Canada

FEDSM-ICNMM2010-30573

A TWO-WAY COUPLED POLYDISPERSED SIMULATION OF BUBBLY FLOW BENEATH A PLUNGING LIQUID JET

Jingsen Ma, Assad A. Oberai*, Donald A. Drew and Richard T. Lahey, Jr
Center for Multiphase Research
Rensselaer Polytechnic Institute
Troy, NewYork 12180.
Email: maj6@rpi.edu, oberaa@rpi.edu, drewd@rpi.edu and laheyr@rpi.edu

ABSTRACT

Plunging liquid jets are commonly encountered in nature and are widely used in industrial applications (e.g., in waterfalls, waste-water treatment, the oxygenation of chemical liquids, etc.). Despite numerous experimental studies that have been devoted to this interesting problem, there have been very few two-phase flow simulations. The main difficulty is the lack of a quantitative model to simulate the air entrainment process, which plays a critical role in this problem. In this paper, we present a computational multiphase fluid dynamics (CMFD) approach for solving this problem. The main ingredients of this approach are a comprehensive subgrid air entrainment model that predicts the rate and location of the air entrainment and a two-fluid transport model in which bubbles of different sizes are modeled as a continuum fluid. Using this approach, a Reynolds-averaged Navier Stokes (RaNS) two-way coupled two-phase flow simulation of a plunging liquid jet with a diameter of 24mm and a liquid jet velocity around 3.5m/s was performed. We analyzed the simulated void fraction and bubble count rate profiles at three different depths beneath the average free surface, and compared them with experimental data. We observed good agreement at all locations.

INTRODUCTION

The plunging liquid jet problem involves the impingement of a liquid jet onto a pool of liquid. It is accompanied by strong air entrainment once the jet velocity exceeds a certain threshold velocity. This process is widely encountered in the nature and various industrial applications. For example, air is entrained by water falls in rivers and by breaking and plunging waves in the sea, during which processes the carry-under of oxygen helps to support aquatic life while the caputure of CO_2 aids in mitigating the green-house effect. In addition, gas entrainment by a plunging liquid jet may be used to enhance the rate of a chemical reaction that occurs at gas/liquid interfaces by increasing the resultant interfacial area. Also, the breaking bow wave around a maneuvering surface ship behaves like a plunging jet and entrains air which may alter the drag characteristics of the ship and influence the optical and acoustic signatures of the ship-hull flow.

Numerous experimental studies have been devoted to the air entrainment and the consequent bubbly flow underneath a plunging liquid jet (see reviews: by Bin [1] and Chanson [2]). In contrast, the body of literature devoted to the two-phase numerical simulation of this problem is quite small. The simulation of the entrainment of air bubbles by a plunging liquid jet and their transport is quite challenging. It is a multiscale problem with very disparate characteristic length and time scales. For example, the smallest bubbles and liquid eddies might be of the order of microns while the jet diameter is often on the order of meters. Given these features it is not surprising that few researchers have performed a Direct Numerical Simulation (DNS) of this problem where the liquid and gas phases were explicitly resolved, though some notable attempts have been made in this direction (e.g., the work of Iafrati et al. [3] and Galimov et al [4,5]). However, these

*Address all correspondence to this author.

simulations were only up to the formation of the first air cavity and the beginning of bubble breakup. This was due to the lack of spatial resolution to resolve the complex gas/liquid interfaces and the computing costs. These difficulties may be overcome by utilizing a Two-Fluid Model (TFM) [6, 7], in which both the continuous liquid and the dispersed gas phases as represented as fluid continua at every spatial location. In this approach individual bubbles are not modeled and the rough gas/liquid interfaces are smoothed out, which eases the computational burden. However, subgrid models for the interaction between the bubbles and liquid as well as for the entrainment of air at the interfaces are required.

Over the years, various subgrid closure models for the interaction between gas bubbles and the continuous liquid have been proposed [6, 7]. These include models for the drag, lift, virtual mass, turbulent dispersion and bubble-wall forces. In contrast few models for subgrid air entrainment have been developed. The notable exceptions are [8, 9]. Our primary work in this area was based on the model proposed by Moraga et al. [10] which predicts the location of air entrainment. In [11] we combined this location-prediction model with an expression for the quantity of air entrained due to a plunging jet to perform one-way coupled (where the forces exerted by the gas on the liquid are neglected) monodisperse simulation of the plunging jet problem. However, the model for the location of air entrainment proposed in [10] has a drawback that it predicts finite entrainment even at a gas/liquid interface that is moving downward with a uniform spatial velocity [12, 13]. Subsequently, we proposed a novel air entrainment model [12, 13] that not only overcomes this drawback in location prediction but also provides the rate of air entrainment for various types of flows, with a quite simple expression. In one-way coupled tests of monodisperse flows this model has provided good results for several free-surface bubbly flows including, plunging liquid jets, hydraulic jumps and ship-hull flows. In this paper we apply this model to a polydisperse, two-way coupled simulation of a plunging liquid jet for the experiments of Chanson et al. [14, 15]. We believe that two-way coupling is necessary because of the high void fractions (up to 20%) observed in this flow, and a polydisperse model is required based on the experimental observations of a wide range of distribution of bubble diameters (from smaller than 1mm to larger than 10mm).

In the next section (Sec. 2) we describe the main features of the two-way coupled, polydispersed two-fluid model and the generalized air entrainment model. After that, in Section 3, we carry out a simulation of a plunging liquid jet induced bubbly flow by utilizing this computational multiphase fluid dynamics (CMFD) framework, and present the predicted results along with a quantitative comparison with the experimental data. Finally, the main conclusions from this study are given in Section 4.

TWO-FLUID MODEL WITH AIR ENTRAINMENT

In this section we describe a RaNS-type, two-fluid, CMFD model, and a subgrid air entrainment model. In contrast to previous studies on plunging liquid jets [11–13] the two-fluid model used herein is two-way coupled and polydispersed.

Mass conservation of the bubble phase

The conservation equation of the bubble number density, N_g''', for bubbles of a characteristic diameter, D_g, moving with a velocity of $\mathbf{u}_g$, is often referred to as a Boltzmann-type population balance equation [16, 17]. It is given by:

$$\frac{\partial N_g'''}{\partial t} + \nabla \cdot \left(\mathbf{u}_g N_g''' \right) = \mathscr{E}_g \tag{1}$$

where $\mathscr{E}_g$ is the rate at which the bubble density increases due to air ingestion at the free surface and is discussed below. Note that other sources of bubbles (e.g., those due to breakup and coalescence) can also be included on the right hand side of Eq. 1 (see [10]) but, for simplicity, were ignored in this study.

The entrained air flux is given by a newly developed sub-grid air entrainment model [12,13]. This model was derived assuming that the turbulence near the air-water interface produces air cavities of size $a \sim k/g$, where k is the turbulence kinetic energy and g is acceleration due to gravity, and that the entrainment rate is proportional to the downward velocity difference between these cavities and the free surface. This argument yields the following expression for the air flux:

$$q(\mathbf{x}) = \frac{C_{ent}}{g} k(\mathbf{x}) \frac{\partial u_n}{\partial n}(\mathbf{x}), \tag{2}$$

where $\mathbf{x}$ is a location near the free surface, q is the volume of air entrained per unit interface area, per unit time, C_{ent} is a model coefficient and $\frac{\partial u_n}{\partial n}$is the normal derivative of the normal component of the liquid velocity at the interface. This model gives the entrained air flux as a volumetric flow rate per unit interfacial area, however, in our two-fluid model the entrained air is distributed as a volume source at the interface in a layer that is ϕ_{ent} thick. Thus the rate of air entrainment per unit volume, per unit time, is:

$$Q(\mathbf{x}) = \frac{q(\mathbf{x})}{\phi_{ent}} = \frac{C_{ent}}{g\phi_{ent}} k(\mathbf{x}) \frac{\partial u_n}{\partial n}(\mathbf{x}), \tag{3}$$

Finally this volume of air is distributed among bubble groups of different diameters. So the number density of bubbles of a given diameter, D_g, per unit volume, per unit time, is given by:

$$\mathscr{E}_g(\mathbf{x}) = \frac{C_{ent}}{\phi_{ent} g} \frac{f_E \Delta D_g}{V_{avg}} k(\mathbf{x}) \frac{\partial u_n}{\partial n}(\mathbf{x}), \tag{4}$$

where $f_E(D_g)$ is the pdf of the source distribution as a function of the bubble diameter, D_g. In practice $f_E(D_g)$ should be prescribed or obtained from the experiments. In a polydisperse model, ΔD_g is the width of the bubble diameter bin and $V_{avg} = \sum_{D_g} f_E(D_g)\bar{v}_g \Delta D_g$ is the average bubble volume of a given bin, where $\bar{v}_g$ is the mean volume of a bubble with diameter D_g.

Momentum balance of the dispersed phase

The ensemble-averaged balance of momentum equation for the dispersed phase is given by [18]:

$$\frac{\partial(\bar{v}_g N_g''' \rho_d \mathbf{u}_g)}{\partial t} + \nabla \cdot (\bar{v}_g N_g''' \rho_d \mathbf{u}_g \otimes \mathbf{u}_g) = \bar{v}_g N_g''' \nabla p_c + \bar{v}_g N''' \rho_d \mathbf{g} + \mathbf{M}_g' \tag{5}$$

where ρ_d is the air density, and p_c is the pressure of the liquid. Note that $\mathbf{M}_g'$, the fluctuating interfacial force density, must be constituted. This term determines momentum transfer between the continuous phase and the dispersed phase. It may be partitioned to account for different types of interactions [6, 19],

$$\mathbf{M}_g' \cong \mathbf{M}_g^{TD} + \mathbf{M}_g^{D} + \mathbf{M}_g^{VM} + \mathbf{M}_g^{L} + \mathbf{M}_g^{W} \tag{6}$$

where the right hand side contains contributions due to turbulent dispersion (TD), drag (D), virtual mass (VM), lift (L) and wall-induced forces (W), respectively. In our simulation the wall-induced forces were set to zero because there are no solid walls in the region of interest. The turbulent dispersion term was also turned off, even though in our previous one-way coupled simulations [11–13] this term was active. The reason behind this will be explained later in Section 3. The other terms that appear in the above equation are the same as given by Moraga et al. [10], with the exception of the bubble drag term. Here we have employed a correction based on the liquid shear rate proposed by Legendreand & Magnaudet [20] and utilized by Hosokawa & Tomiyama [21].

Mass conservation of the continuous phase

The continuity equation for the liquid phase is [6],

$$\frac{\partial \alpha_c \rho_c}{\partial t} + \nabla \cdot \alpha_c \rho_c \mathbf{u}_c = 0 \tag{7}$$

where $\mathbf{u}_c$, and ρ_c are the ensemble-averaged velocity and density for the continuous phase (i.e., the liquid). Also, α_c is the liquid volume fraction, which satisfies:

$$\alpha_c = 1 - \alpha = 1 - \sum_{g=1}^{G} \alpha_g \tag{8}$$

where α_g is the void fraction for group g and related to the number density by $\overline{v_g} N_g'''$, and α is the total void fraction.

Momentum conservation of the continuous phase

Conservation of momentum for the continuous phase in the average sense is expressed as [6],

$$\frac{\partial \alpha_c \rho_c \mathbf{u}_c}{\partial t} + \nabla \cdot \alpha_c \rho_c \mathbf{u}_c \mathbf{u}_c = \nabla \cdot \alpha_c (\mathbf{T}_c + \mathbf{T}_c^{Re}) + \alpha_c \rho_c \mathbf{g} - \sum_{g=1}^{G} \mathbf{M}_g \tag{9}$$

where $\mathbf{T}_c$ is the stress tensor and $\mathbf{T}_c^{Re}$ is the Reynolds stress tensor for the continuous phase. The stress tensor is given by $\mathbf{T}_c = -p_c \mathbf{I} + 2\mu_c \mathbf{D}_c$ and the Reynolds stress tensor is modeled as,

$$\mathbf{T}_c^{Re} = -(\frac{2}{3}\rho_c k)\mathbf{I} + 2\mu_t \mathbf{D}_c \tag{10}$$

where $\mathbf{I}$ is the identity tensor, μ_c is the liquid viscosity, $\mathbf{D}_c$ is the rate of strain of the liquid phase, k and μ_t are the turbulent kinetic energy and the liquid's turbulent viscosity, respectively. In this work, the blended $k-\omega$ /$k-\varepsilon$ turbulence model developed by Menter [22], associated with corrections due to bubble-induced turbulence generation and dissipation, was used to determine k and μ_t and hence to construct $\mathbf{T}_c^{Re}$. All the model coefficients used herein are the same as used previously [10].

Modeling the free surface

The free surface of the air/water mixture was represented using a single-phase level set function ϕ [23], which is the signed distance from the interface, where the level set $\phi = 0$ representing the free surface. Its evolution is governed by:

$$\frac{\partial \phi}{\partial t} + \mathbf{u_c} \cdot \nabla \phi = 0 \tag{11}$$

For more details on the application of the single-phase level set method to bubbly flow simulations the reader is referred to the work of Carrica et al. [24, 25] and Moraga et al. [10].

NUMERICAL SIMULATION

Using our new air entrainment model and the two-fluid multiphase CMFD model described above, we have simulated a plunging liquid jet and compared our results with the experiments of Chanson et al. [14, 15], where both void fraction and bubble count rate distributions were presented. In addition, we have investigated the effect of two-way coupling on our results by comparing two-way and one-way coupled simulations.

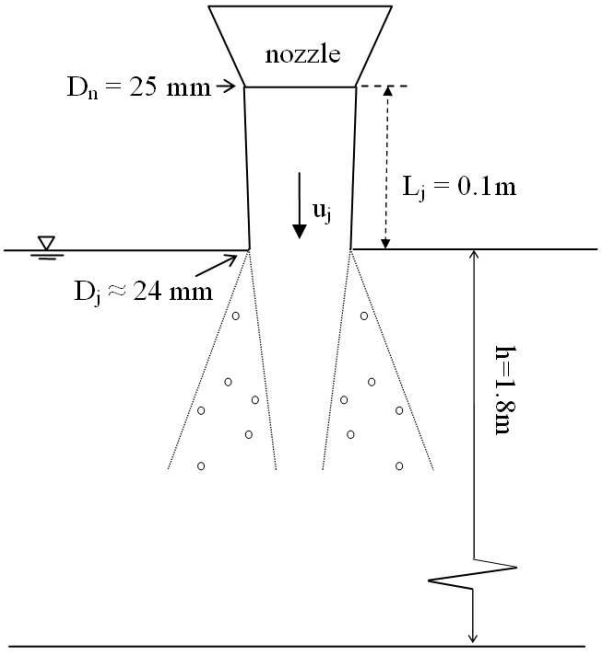

FIGURE 1. Schematic diagram of experimental set-up [14, 15]

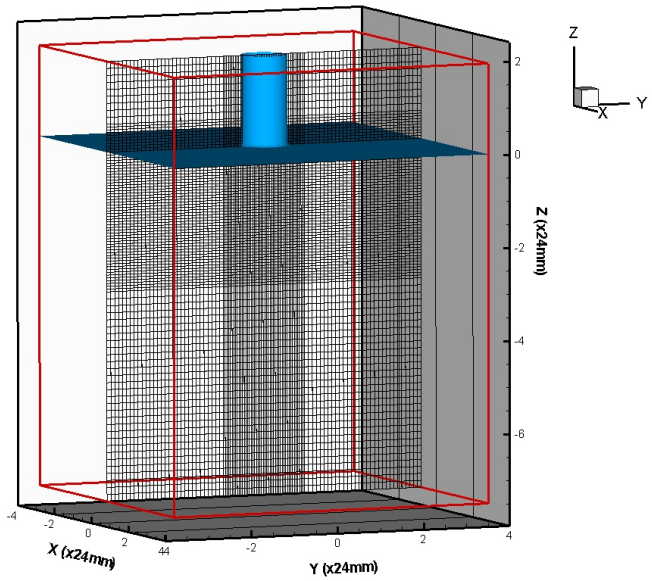

FIGURE 2. Computational domain and mesh, where the dark horizontal surface represents the free surface

Experimental and simulation setup

A schematic view of Chanson's experiment is shown in Fig. 1. A liquid jet of water issuing from a nozzle with a diameter, D_n, of 25mm was allowed to fall vertically under gravity into a pool of stationary water that was 1.8m deep, 0.3m in width and 3.6m in length. The liquid jet began its fall 0.1m above the free surface of the pool. The case studied here has an impact liquid jet velocity at the free surface (u_j) of 3.5m/s, with an estimated liquid jet diameter at impact of $D_j = 24$ mm. Void fraction and bubble count rate measurements were made along planes that were at a depth of 0.8 D_j, 1.2 D_j, 2.0D_j from the free surface.

In the numerical simulation a smaller computational domain was utilized, as shown in Fig. 2, which was large enough so that the boundaries had no influence on the center region where the bubbles were present [11–13]. The two-fluid equations were nondimensionalized using the liquid jet diameter and the liquid velocity at the top of computational domain (i.e. 50 mm above the free surface), which were set to produce the right value of D_j and u_j at the impact surface and led to a Reynolds number of approximately $81,000$.

On every surface of the computational domain, boundary conditions were needed for the three liquid and gas velocity components, the pressure, the gas number density, the level set function, the turbulent kinetic energy, k, and the specific dissipation rate, ω. On the top surface, in order to model the liquid jet, the vertical component of the liquid velocity was set to -1 within a circle of unit diameter. All other liquid and gas velocity components and the bubble number density function were set to zero. A zero-gradient boundary condition was selected for pressure, while the level set function was selected such that its zero coincided with the periphery of the liquid jet and its value elsewhere was set equal to the signed distance from the zero level set. The turbulent model variables, k and ω, were set to their free-stream values of $9 \times 10^{-4}/Re$ and 0.9, respectively, and verified to be small enough to not influence the results in this study. On the four vertical boundaries the zero gradient boundary condition was used for all variables. On the bottom surface the piezometric pressure was set to zero [26], and a zero gradient boundary condition was used for all other variables. For the initial condition all velocities, the pressure and the number density function were set to zero and the level set function was set to the signed distance from the interface.

A structured grid consisting of 1,166,400 cells in total (shown in Fig. 2), which was verified to be fine enough to ensure the grid convergence [11], was used in the simulations. In the region of interest, which included the impact region and the region where void fraction and bubble count rate measurements were made, the grid size was set to $(l_x, l_y, l_z) = (0.04, 0.04, 0.06)$. Outside this region the grid was roughly 2.5 times as coarse.

Simulation results

The simulations were started by modeling the liquid phase only and a statistically stationary solution was obtained after 2,000 time steps with a non-dimensional time step of 0.015 (i.e., a dimensional time-step of around 0.1 ms). This solution for the single-phase flow (water) was then used as an initial con-

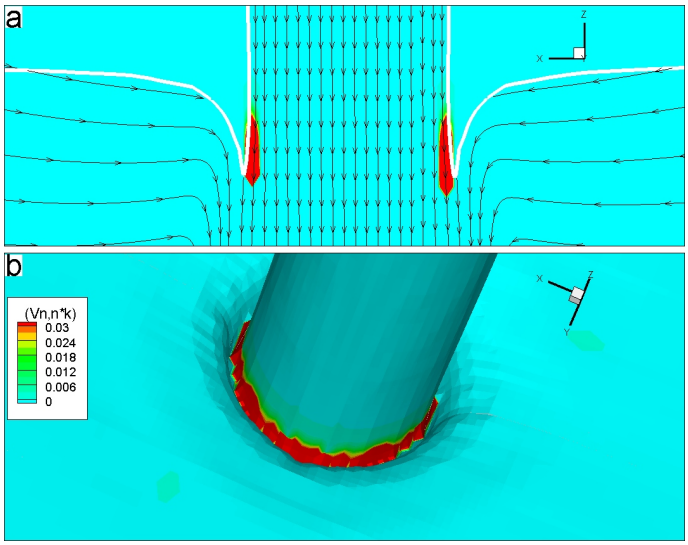

FIGURE 3. Distribution of the kernel of the entrainment source strength, $k\frac{\partial u_n}{\partial n}$, for the plunging jet problem with $u_j = 3.5m/s$: (a)slice through center of the jet, where the white line represents the free surface; (b)three-dimensional view of the free surface.

dition for the simulation of bubbly flow, which was activated by turning on the air entrainment model, with $\phi_{ent} = 0.05\ D_j$ and $C_{ent} = 1.4 \times 10^{-2}$ in this air entrainment model. We employed 5 groups of bubbles having diameters of 1mm, 3mm, 5mm, 7mm and 9mm, respectively, with a probability of 34.78%, 17.39%, 13.04%, 8.70% and 17.39%, respectively. This set of bubble sizes and probabilities were estimated from Fig. 6b in the report of Chanson et al. [15], which gives the probability density function (PDF) of the pseudo-bubble chord lengths (i.e., the product of the measured chord time and the liquid jet velocity).

This polydispersed bubbly flow simulation was carried out with the same time step used previously. After about 600 time steps, during which period the gas phase achieved a quasi-steady distribution in the region of interest (i.e., from the impact surface to $2D_j$ below it), where void fraction data were available. We started collecting void fraction data at this instant and averaged them in time. The time-averaged void fraction were found to attain a statistically stationary value after another 3000 time steps. These time-averaged results were then further averaged in the circumferential direction around the liquid jet. The experimental results [14,15] were measured along a horizontal line that passed through the center of the plunging liquid jet. Since the measurements were expected to be symmetric about the center of the jet, results from either side of the center-line were averaged in order to reduce experimental uncertainty. These averaged results were then compared with the averaged simulation results.

We first examine the rate of air entrainment by plotting, in Fig. 3, the kernel of the air entrainment model given in Eqn. 4 , $k\frac{\partial u_n}{\partial n}$. We observe that air was strongly entrained close to the

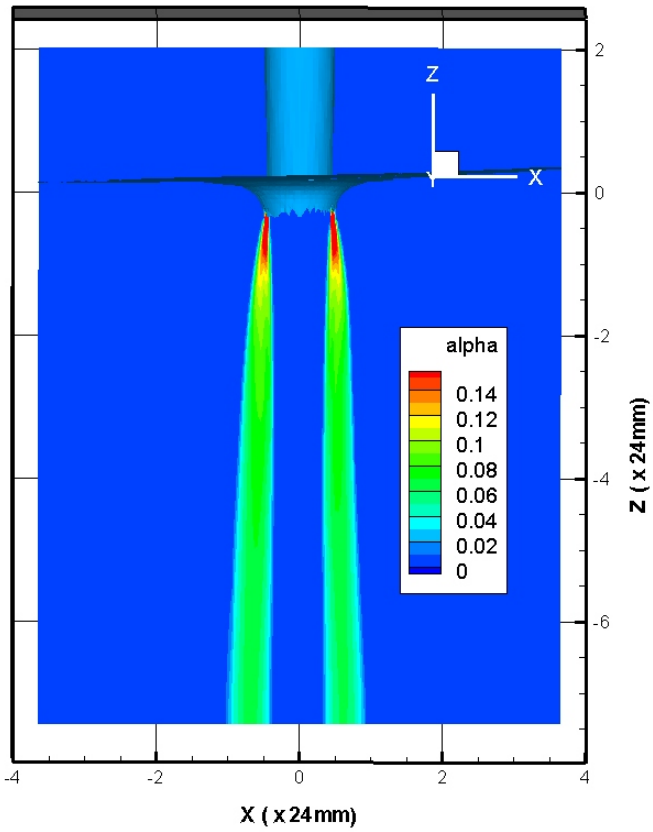

FIGURE 4. A typical snapshot of void fraction distribution.

free surface along the perimeter of the liquid jet. In this region, liquid that is flowing radially inward toward the center of the jet impinges on liquid carried by the jet (see the streamlines in Fig. 3 (a)). This leads to a negative value of the surface divergence, which implies a positive value of $\frac{\partial u_n}{\partial n}$. This in turn implies that any air pockets created near the free surface in this region will be entrained. This is consistent with the results and observations reported in experiments [15, 27]. After bubbles were entrained along the perimeter of the jet, they are convected downward. With increasing depth these bubbles disperse radially, forming an annular region whose thickness increases with depth. This is clearly seen in Fig. 4, which is a snapshot of void fraction obtained from a typical two-way coupled run.

To study the effect of the gas/liquid couplings, we present, in Fig.5, a zoomed-in view of the region close to the free surface. In particular, we plot the predicted void fraction contours for four cases: (a) two-way coupling simulation with turbulent dispersion; (b) two-way coupling simulation without turbulent dispersion; (c) one-way coupling simulation with turbulent dispersion; (d) one-way coupling without turbulent dispersion. We observe that the (b) and (c) cases present similar results that are consistent with each other and physical observations, while the

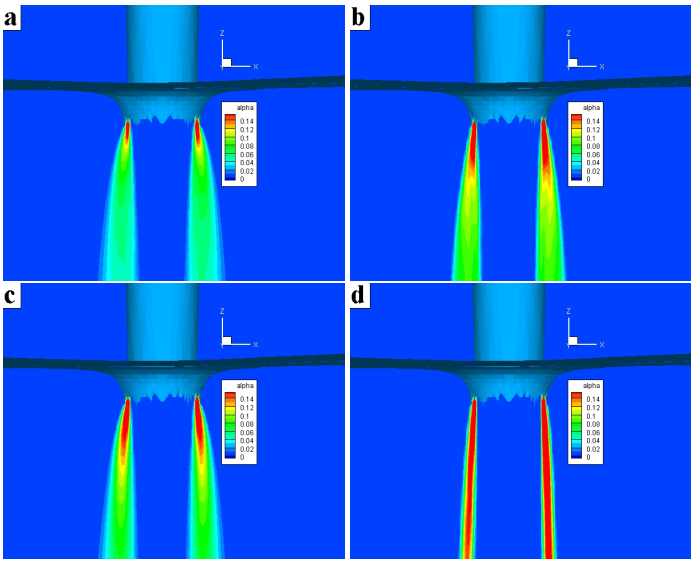

FIGURE 5. A Comparison of void fraction contours predicted by: (a) two-way coupling simulation with turbulent dispersion; (b) two-way coupling simulation with the turbulent dispersion model inactive; (c) one-way coupling with the turbulent dispersion model turned on; (d) one-way coupling with the turbulent dispersion model inactive.

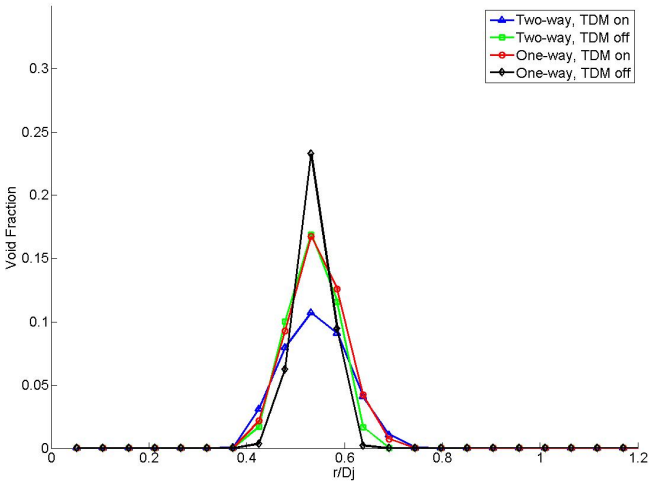

FIGURE 6. A Comparison of the void fraction profiles at $0.8D_j$, predicted in 4 cases.

one-way coupled simulation without turbulent dispersion misses the spreading of the void fraction profile with increasing depth thus resulting in a very sharp void fraction profile. In contrast the two-way coupled results with turbulent dispersion overpredicts the spreading effect so that it causes the void fraction profile too flat. All of these can be further exhibited in Fig.6. This interesting phenomenon may be explained as follows, in the two-way coupled simulations the dispersed phases exert lift and drag reaction forces on the liquid. The lift force imparts a radial velocity to the liquid stream whereas the drag force lowers its downward component. The increased radial liquid velocity then spreads out the bubble distribution radially, and the reduced downward velocity further increases the rate of spreading with depth. Thus for a two-way coupled modeling, a turbulent dispersion model is not needed. However, in a one-way coupled simulation both these effects on the liquid velocity are not captured, and thus the bubbles are convected downward rapidly with minimal spreading. So a turbulent dispersion model should be used to enhance the spreading in one-way coupled simulations. Indeed when this term is turned on, a distribution that is similar to the two-way coupled case is obtained.

Next we compare the total void fraction distributions with the experimental data in Fig.7. Each plot contains both experimental and predicted void fraction profiles (for two-way coupling) as a function of the normalized radial coordinate, where $r = 0$ represents the centerline of the liquid jet. The measurement depths for the top, the center and the bottom plot are equal to $0.8D_j$, $1.2D_J$ and $2.0D_j$, respectively. For the plot on the top, which corresponds to a depth of $h = 0.8D_j$ and is quite close to the free surface, it can be seen that there is good agreement in the location and magnitude of the peak void fraction between the experiment and the simulation. This indicates that the air entrainment model is able to accurately capture the location and strength of the air sources. As we move down to the two lower depths, though some deviation is observed, the agreement between the experiment and the simulation results remains good. This indicates that a two-way coupled two-fluid model correctly models the spreading of the two-phase jet and the transport of bubbles once they are entrained. In addition, it's worthy of mention that our results also match the analytical solution predicted by the simplistic diffusion model suggested by Chanson [27]. Similar results can also be obtained using a one-way coupled simulation with the aid of a turbulent dispersion model [11–13].

Another challenging test of the two-fluid model is to examine its ability to predict the polydispersed properties of bubbly flows. One such property is the bubble count rate, or bubble frequency, which is experimentally defined as the number of bubbles impacting a probe per unit time during the measurements. The local bubble count rate was related to the local total air content, average velocity and bubble mean chord length [14] as:

$$F = \frac{\alpha \bar{\mathbf{u}}_g}{ch_{mean}} \tag{12}$$

Based on this equation, the total local air volume fraction and the local bubble velocities predicted by the simulation, we are able to reproduce the bubble count rate profiles for plunging liquid jets, if we know the mean chord length, ch_{mean}, of the bubbles.

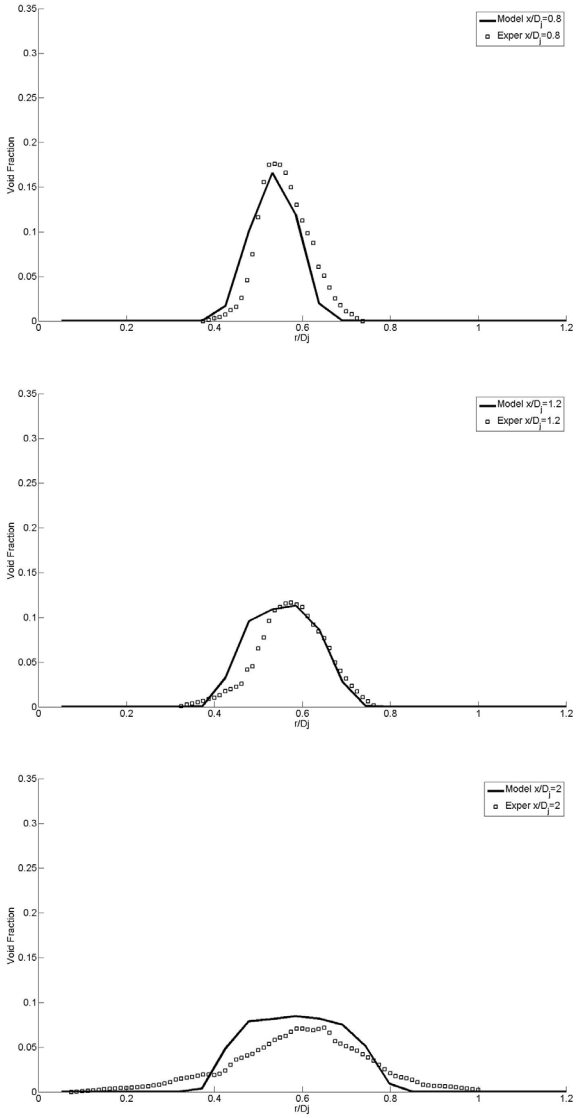

FIGURE 7. Temporally and circumferentially-averaged void fraction profiles at $0.8D_j$ (top), $1.2D_j$(middle), $2.0D_j$(bottom)

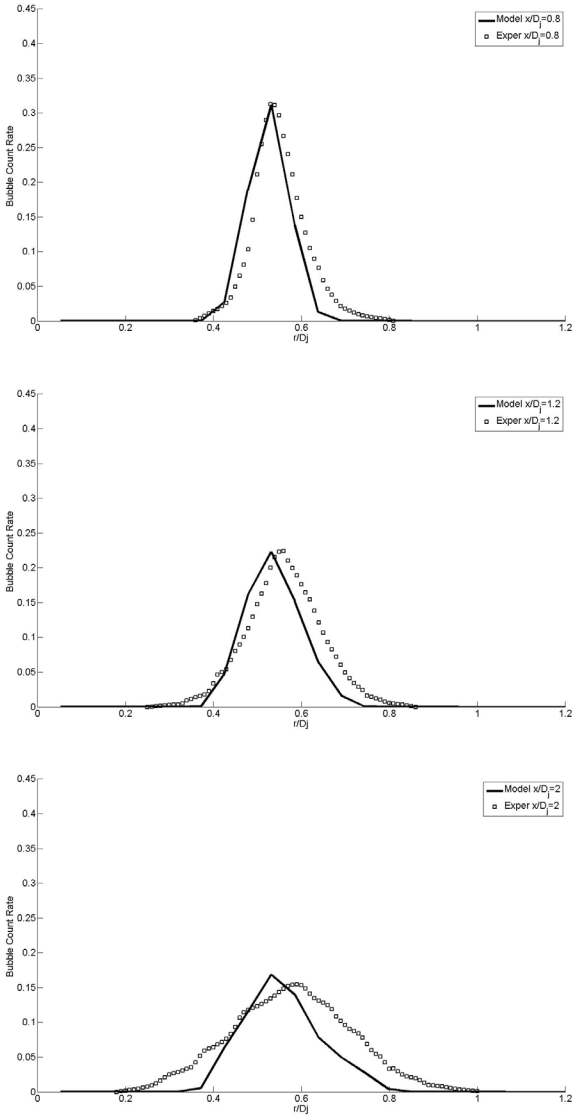

FIGURE 8. Temporally and circumferentially-averaged bubble count rate profiles at $0.8D_j$ (top), $1.2D_j$(middle), $2.0D_j$(bottom)

However, in the experiments of Chanson et al. [14, 15], the local bubble velocity was not measured, thus ch_{mean} could not be obtained directly. Therefore, we calculated the local averaged bubble diameters, $D_{g_{mean}}$, and use it to replace ch_{mean} in Eq. 12, to obtain the local bubble count rate. Fig. 8 displays both the calculated and measured bubble count rate profiles for three different depths. From the figure we observe that our simulation reproduces the experimental measurements reasonably well. This implies that our two-way coupled simulation correctly captures the polydispersed properties of the bubbly flow.

CONCLUSIONS AND DISCUSSION

By incorporating a novel, generalized subgrid air entrainment model, a two-way coupled, polydispersed, two-fluid model for modeling free-surface bubbly flows was developed. Using this approach a polydispersed simulation for a plunging liquid jet was done. Five groups of bubbles with diameters raging from 1mm to 9mm were employed. Both the predicted void fraction profiles and bubble count rates were compared with experimental data and good agreement was found. To our knowledge, this is the first quantitative numerical prediction of both gas concentrations and bubble count rates in the bubbly flow underneath a

plunging liquid jet.

The difference between one-way and two-way coupled simulations was also analyzed. It was found that a turbulent dispersion model was needed for one-way coupled simulations, but not when there was two-way coupling. This was attributed to the force exerted by the bubbles on the liquid that enhances its radial velocity and retards its downward velocity. These forces are inherently present in two-way coupled simulations but absent in one-way coupled simulations. This suggests that in some instances a two-way coupled CMFD model leads to a better and simpler characterization of the interphase momentum transfers by avoiding the use of a phenomenological turbulent dispersion model.

ACKNOWLEDGMENT

This work was supported by the Office of Naval Research(ONR), Grant N00014-03-1-0826, under the administration of Dr. Patrick Purtell, and was also supported in part by a grant of computer time from the DOD High Performance Computing Modernization Program at the Maui High Performance Computing Center (MHPCC), US Army Engineering and Research Development Center (ERDC) and US Army Research Laboratory(ARL).

REFERENCES

[1] Bin, A., 1993. "Gas entrainment by plunging liquid jets". *Chemical Engineering Science,* ***48***(21), pp. 3585–3630.

[2] Chanson, H., 1996. *Air Bubble Entrainment in Free-Surface Turbulent Shear Flows*. Academic Press.

[3] Iafrati, A., Campana, E. F., Gomez Ledesma, R., Kiger, K. T., and Duncan, J. H., 2004. "Air entrainment induced by the impact of a planar translating jet on a flat free surface". Proc. 25th Symposium on Naval Hydrodynamics, ***3***, p. 84.

[4] Galimov, A., 2007. "An analysis of interfacialwaves and air ingestion mechanisms". PhD thesis, Rensselaer Polytechnic Institute.

[5] Galimov, A. Y., Sahni, O., Jr., R. T. L., Shephard, M. S., Drew, D. A., and Jansen, K. E., 2010. "Parallel adaptive simulation of a plunging liquid jet". *Acta Mathematica Scientia,* ***30***(2), pp. 522 – 538.

[6] Drew, D., and Passman, S., 1998. *Theory of multicomponent fluids*, Vol. 135 of *App. Math. Sci.* Springer.

[7] Lahey, Jr., R. T., 2009. "On the computation of multiphase flow". *J. Nuclear Technology,* ***167***, pp. 1–17.

[8] Souders, D. T., and Hirt, C. W., 2004. "Modeling entrainment of air at turbulent free surfaces". In Proceedings of The 2004 World Water and Environmental Resources Congress .

[9] Shi, F., Kirby, J., Haller, M., and Catal, P., 2008. "Modeling of surfzone bubbles using a multiphase vof model". In Proceedings of the 31st International Conference on Coastal Engineering.

[10] Moraga, F. J., Carrica, P. M., Drew, D. A., and Lahey, Jr., R. T., 2008. "A subgrid air entrainment model for breaking bow waves and naval surface ships". *Computers & Fluids,* ***37***(3), pp. 281 – 298.

[11] Ma, J., Oberai, A., Drew, D., Lahey Jr, R., and Moraga, F., 2010. "A quantitative subgrid air entrainment model for bubbly flows-plunging jets". *Computers & Fluids,* ***39(1)***, pp. 77–86.

[12] Ma, J., Oberai, A., Drew, D., Lahey Jr, R., and Hyman, M., 2010. "A comprehensive subgrid air entrainment model for RaNS modeling of bubbly flows near the free surface". *submitted to Computers & Fluids*.

[13] Ma, J., Oberai, A., Drew, D., Lahey Jr, R., and Hyman, M., 2009. "A comprehensive subgrid air entrainment model for Reynolds-averaged simulations of free-surface bubbly flows". In APS DFD Meeting Abstracts.

[14] Chanson, H., Aoki, S., and Hoque, A., 2002. Similitude of air bubble entrainment and dispersion in vertical circular plunging jet flows: An experimental study with freshwater, salty freshwater and seawater. Coastal/Ocean Engineering Report COE02-1, Dept. of Architecture and Civil Eng., Toyohashi University of Technology, Japan.

[15] Chanson, H., Aoki, S., and Hoque, A., 2004. "Physical modelling and similitude of air bubble entrainment at vertical circular plunging jets". *Chemical Engineering Science,* ***59***(4), pp. 747 – 758.

[16] Martinez-Bazan, C., Montañes, J., and Lasheras, J. C., 1999. "On the breakup of an air bubble injected into a fully developed turbulent flow. Part 1. Breakup frequency.". *J. Fluid Mechanics,* ***401***, pp. 157–182.

[17] Larreteguy, A. E., Drew, D. A., and Lahey, Jr., R. T., 2002. "A center-averaged two-fluid model for wall-bounded bubbly flows.". In Proc. 2002 Joint US ASME/European Fluids Engineering Division Summer Meeting.

[18] Moraga, F., Larreteguy, A., Drew, D., Lahey, R., et al., 2006. "A center-averaged two-fluid model for wall-bounded bubbly flows". *Computers & Fluids,* ***35***(4), pp. 429–461.

[19] Lahey, Jr., R. T., 2005. "The simulation of multidimensional multiphase flows". *Nuclear Engineering and Design,* ***235***, pp. 1043–1060.

[20] Legendre, D., and Magnaudet, J., 1998. "The lift force on a spherical bubble in viscous linear flow". *J. Fluid Mechanics,* ***368***, pp. 81–126.

[21] Hosokawa, S., and Tomiyama, A., 2009. "Multi-fluid simulation of turbulent bubbly pipe flows". *Chemical Engineering Science,* ***64***(24), pp. 5308 – 5318.

[22] Menter, F. R., 1994. "Two-equation eddy viscosity turbulence models for engineering applications.". *AIAA Journal,* ***32***(8), pp. 1598–1605.

[23] Sussman, M., Smereka, P., and Osher, S., 1994. "A level set approach for computing solutions to incompressible two-phase flow". *Journal of Computational Physics,* ***114***(1), September, pp. 146–159.

[24] Carrica, P. M., Wilson, R. V., and Stern, F., 2006. "An unsteady single-phase level set method for viscous free surface flows". *Int. J. Num. Meth. Fluids,* ***53***, pp. 229–256.

[25] Carrica, P. M., Wilson, R. V., and Stern, F., 2006. "Unsteady RaNS simulation of the ship forward speed diffraction problem". *Computers & Fluids,* ***35***, pp. 545–570.

[26] Paterson, E. G., Wilson, R. V., and Stern, F., 2003. General-purpose parallel unsteady rans ship hydrodynamics code: CFDShip-Iowa. IIHR Report 432, Iowa Institute for Hydraulic Research. The University of Iowa, Iowa, USA.

[27] Chanson, H., 1996. "Air entrainment by plunging jets". In *Air Bubble Entrainment in Free-Surface Turbulent Shear Flows*. Academic Press, San Diego, pp. 53 – 72.